Non-uniform Planar MIMO Array Optimization Criterion in Wavenumber Domain for Aliasing-free Wideband Near-Field 3D Imaging

Mingsai Huan[(1)], Yugang Ma[(2)], Shuoguang Wang[(3)], Junli Liang[(1)], Yonghong Zeng[(2)], and Francois Chin[(2)]

[(1)] Northwestern Polytechnical University, Xi'an Shaanxi, China (huanmingsai@163.com)
[(2)] Institute for Infocomm Research, Agency for Science, Technology and Research, Singapore
[(3)] Academy for Network & Communications of CETC, Shijiazhuang Hebei, China.

***Abstract*—Microwave/millimeter-wave imaging is widely desired in various applications, including remote sensing, integrated sensing and communications, security, and biomedical imaging. Sparse MIMO arrays, while cost-effective, often face aliasing artifacts due to spectral distortion in non-uniform sampling. This paper introduces an innovative optimization criterion for non-uniform planar MIMO arrays in the wavenumber domain, aiming at aliasing-free wideband near-field 3D imaging. We propose the wavenumber-range spectrum (WS) of the normal plane wave as a tool to evaluate spectral distortion in near-field non-uniform sampling. This approach utilizes the non-uniform-fast-Fourier-transform-based MIMO range migration algorithm with a modified non-uniform sampling function. Simulations show that the array, with maximum peak sidelobe ratio (PSLR) in the WS, consistently maintains low PSF sidelobe levels for central and edge targets, and thus achieves aliasing-free imaging.**

I. Introduction

Microwave/Millimeter-wave imaging is integral to diverse applications including remote sensing, concealed weapon detection, target identification, nondestructive testing, scattering diagnosis, vibration analysis, biomedical imaging, and through-the-wall radar imaging. Planar multiple-input multiple-output (MIMO) arrays with wideband signals, using fewer antenna elements than monostatic arrays, offer a cost-effective approach for high-resolution 3D imaging [1].

Sparse MIMO arrays further reduce costs but risk significant aliasing artifacts, depending on the geometry of antennas. Various techniques have been developed to mitigate these artifacts and improve image quality, though they may distort the target image, increase computational/system costs, or lack generalizability [2]. One approach involves designing non-uniform arrays optimized for a low sidelobe level (SLL) in the point spread function (PSF). However, the PSF-based method is unreliable, and struggles to maintain low-SLL for off-center targets due to the space-shift-variant property of the PSF, presenting challenges in designing non-uniform arrays that effectively suppress aliasing across the entire region of interest.

Recently, [3] introduces a convex optimization model for MIMO array design using compressed sensing to make the combined 2D PSF of sparse arrays closely match that of full arrays. But this method faces computational challenges in 3D imaging due to the complexity of 3D PSF. To address the PSF challenge, [2], building on the k-space analysis in [4], applies minor random displacements to the element positions of sparse periodic arrays. This creates a non-uniform array that prevents coherent accumulation of aliasing components. However, these studies primarily focus on k-space analysis of aliasing in sparse periodic (uniform) arrays, and do not develop a method for evaluating aliasing in non-uniform arrays.

In this paper, the WS of the normal plane wave is introduced as a novel optimization criterion for aliasing-free non-uniform planar MIMO array design. This spectrum is obtained by implementing the non-uniform-fast-Fourier-transform-based MIMO range migration algorithm (NUFFT-based MIMO-RMA) on a modified sampling function, and its PSLR can serve as a indicator for evaluating the degree of aliasing.

II. Wavenumber-range Spectrum

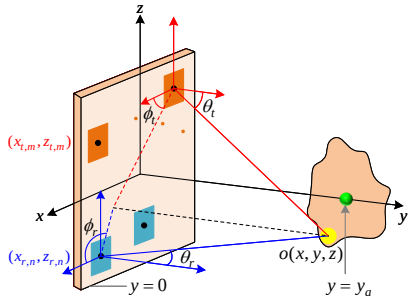


Fig. 1. A planar MIMO array model for wideband near-field 3D imaging.

According to [1], [5], the object's image can be reconstructed via the MIMO-RMA:

$$\hat{o}(x,y,z) = -\frac{1}{2\pi^3}\iiint \frac{k_{y_t}k_{y_r}}{P(k)} S\left(k, k_{x_t}, k_{z_t}, k_{x_r}, k_{z_r}\right) \cdot e^{\mathrm{j}(k_x x + k_y y + k_z z)} \mathrm{d}k_x \mathrm{d}k_y \mathrm{d}k_z, \quad (1)$$

where $k = \frac{2\pi f}{c}$ is the wavenumber, and $P(k)$ is the Fourier spectrum of the wideband signal. $k_{x_t}, k_{z_t}, k_{x_r}, k_{z_r}$ are the Fourier counterparts of element positions x_t, z_t, x_r, z_r in the wavenumber domain. $k_{y_t} = \sqrt{k^2 - k_{x_t}^2 - k_{z_t}^2}, k_{y_r} = \sqrt{k^2 - k_{x_r}^2 - k_{z_r}^2}$, $k_x = k_{x_t} + k_{x_r}$, $k_y = k_{y_t} + k_{y_r}$ and $k_z = k_{z_t} + k_{z_r}$. The NUFFT-based MIMO-RMA [5] can be summarized as follows. **1.** To obtain the 5D spectrum $S\left(k, k_{x_t}, k_{z_t}, k_{x_r}, k_{z_r}\right)$ from the radar measurements $s\left(t, x_t, z_t, x_r, z_r\right)$, a 1D FFT with respect to t and two 2D

spatial NUFFTs over the transmitting and receiving arrays are performed. $\frac{k_{y_t} k_{y_r}}{P(k)}$ acts as a low-pass filter and eliminates the influence of the transmitted signal's spectrum. **2.** Then, a data mapping from 5D grid $S(k, k_{x_t}, k_{z_t}, k_{x_r}, k_{z_r})$ to 3D grid $S(k_x, k_y, k_z)$ is implemented to facilitate the application of the inverse Fourier transform. **3.** Finally, a 1D NUIFFT along the k_y dimension followed by a 2D IFFT along k_x and k_z is performed to finish the image reconstruction.

Since the MIMO-RMA [1] is derived based on the continuous Fourier transform (FT), the results of the FFT for dense uniform arrays well approximate those of the FT. However, for non-uniform arrays, the results of the NUFFT significantly differ from those of the FT (depending on the array geometry), which is the fundamental cause of imaging aliasing in non-uniform arrays. The aliasing primarily depends on the degree of distortion in the spectrum $S(k_x, k_z, k_y)$, and is also affected by the NUIFFT along the k_y dimension.

The spectrum of the sampling function is a recognized metric for evaluating the degree of spectral distortion in non-uniform sampling [6]. The 4D sampling function for non-uniform planar MIMO arrays can be formulated as

$$smp_4(x_t, z_t, x_r, z_r) = \sum_{m=1}^{M} \sum_{n=1}^{N} \delta(x_t - x_{t,m}, z_t - z_{t,m}, x_r - x_{r,n}, z_r - z_{r,n}), \quad (2)$$

where $\delta()$ is the unit impulse signal with $\delta(0,0,0,0) = 1$ and $\delta() = 0$ elsewhere. The physical significance of (2) is that each channel of the MIMO array receives a signal with a value of 1, indicating that the signals across all channels are in phase with each other. This characteristic is a typical property of a normal plane wave. To simulate the phase variation of a normal plane wave with distance, especially for modeling the echo from a target at a distance of y_a, (2) is modified as

$$smp_5(k, x_t, z_t, x_r, z_r) = e^{-\mathrm{j}2ky_a} \cdot smp_4(x_t, z_t, x_r, z_r) \quad (3)$$

Unlike the far-field case [7], under near-field conditions, there is not a direct Fourier Transform relationship between the array element positions and the imaging results. Therefore, we develop a new spectrum of the modified sampling function to evaluate the near-field imaging performance of non-uniform arrays. This specific spectrum is computed via the steps in the NUFFT-based MIMO-RMA that involve non-uniform sampling: **1.** Perform two 2D spatial NUFFTs on (3) over transmitting and receiving arrays to obtain $SMP_5(k, k_{x_t}, k_{z_t}, k_{x_r}, k_{z_r})$. For small-scale imaging, the amplitude factors $k_{y_t} k_{y_r}$ are negligible. **2.** Map data from the 5D grid to a 3D grid, yielding $SMP_3(k_x, k_y, k_z)$. **3.** Execute a 1D NUIFFT along k_y to obtain the wavenumber-range spectrum $WS(k_x, k_z, y)$ of the normal plane wave.

Fig. 2 presents two cross-sections of the WS amplitude pattern of a dense uniform planar MIMO array with 2601 transmitters and 2601 receivers. The pattern closely resembles the shape of a 3D sinc function, with a unique main lobe existing at $(k_x = 0, k_z = 0, y = y_a)$. Therefore, to approach the performance of the uniform array, the PSLR of WS for non-uniform arrays is expected to be maximized. With simulation parameters identical to those in [3], the optimized 4T16R array element positions via sequential quadratic programming [7] and the 3D PSFs for a center target and edge target are shown in Fig. 3. The cross range SLL is -21.1dB for the center target and -24.4dB for the edge, which is lower than the results given in [3]. The range SLL for 3D imaging is about -14dB, which could potentially be reduced further through advanced optimization techniques developed in the future.

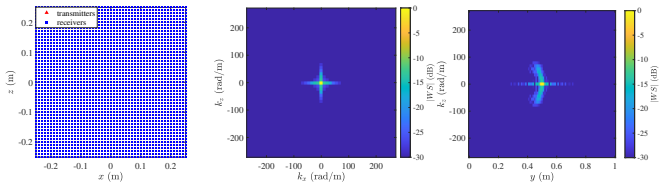


Fig. 2. The element positions of the uniform 2601T2601R array and the WS amplitude cross-sections with $y_a = 0.5$m. The array aperture is 0.5m×0.5m, and the element spacing is 0.01m for signals in the 3-9 GHz frequency range.

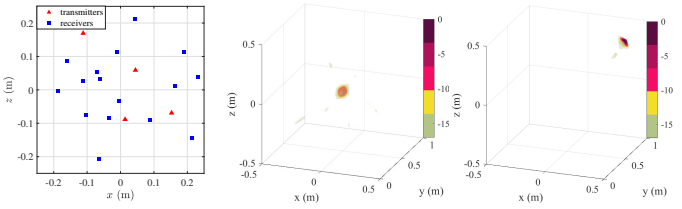


Fig. 3. The element positions of the optimized non-uniform 4T16R array and the 3D PSFs for a center target at (0,0.5,0) and edge target at (0.5,0.5,0.5).

III. Conclusions

The simulations indicate that the optimized non-uniform array consistently maintains low SLL in the PSF for central and edge targets, and hence the PSLR of WS is a reliable metric for quantifying the extent of aliasing.

References

[1] X. Zhuge and A. G. Yarovoy, "Three-dimensional near-field MIMO array imaging using range migration techniques," *IEEE Trans. Image Process.*, vol. 21, no. 6, pp. 3026–3033, Jun. 2012.

[2] M. Kazemi, Z. Kavehvash, M. Shabany, and B. Shamsi, "Aliasing artifacts suppression in MIMO millimeter-wave imaging systems based on k-space analysis," *IEEE Trans. Instrum. Meas.*, vol. 71, pp. 1–9, 2022.

[3] S. Wang, S. Li, A. Hoorfar, K. Miao, G. Zhao, and H. Sun, "Compressive sensing based sparse MIMO array synthesis for wideband near-field millimeter-wave imaging," *IEEE Trans. Aerosp. Electron. Syst.*, pp. 1–16, 2023.

[4] M. Kazemi, Z. Kavehvash, and M. Shabany, "K-space analysis of aliasing in millimeter-wave imaging systems," *IEEE Trans. Microw. Theory Tech.*, vol. 69, no. 3, pp. 1965–1973, Mar. 2021.

[5] J. Wang, P. Aubry, and A. Yarovoy, "3-D short-range imaging with irregular MIMO arrays using nufft-based range migration algorithm," *IEEE Trans. Geosci. Remote Sens.*, vol. 58, no. 7, pp. 4730–4742, Jul. 2020.

[6] F. Marvasti, Ed., *Nonuniform Sampling: Theory and Practice*, ser. Information Technology: Transmission, Processing, and Storage. Boston, MA: Springer US, 2001.

[7] M. Huan, J. Liang, Y. Wu, Y. Li, and W. Liu, "SASA: super-resolution and ambiguity-free sparse array geometry optimization with aperture size constraints for MIMO radar," *IEEE Trans. Antennas Propag.*, vol. 71, no. 6, pp. 4941–4954, Jun. 2023.